Subtropical anticyclone impacts life-history traits of a marine top predator

Ruijiao Sun[1,2,3], Etienne Rouby[1], Henri Weimerskirch[4], Christophe Barbraud[4], Karine Delord[4], Caroline C. Ummenhofer[1], Stéphanie Jenouvrier[1]

*CCU and SJ are co-senior authors

1. Woods Hole Oceanographic Institution, Woods Hole, MA 02543, USA

2. Department of Earth, Atmospheric and Planetary Science, Massachusetts Institute of Technology, Cambridge, MA 02139, USA

3. Marine Science Institute, University of California Santa Barbara, Santa Barbara, CA, USA

4. Centre d'Etudes Biologiques de Chizé, CNRS-La Rochelle University UMR7372, 79360 Villiers en Bois, France

Corresponding Author: Ruijiao Sun

E-mail: ruijiaos@ucsb.edu

Open Research Statement: Data and code can be accessed in GitHub through this link during reviewing processes. If the paper is accepted for publication we will deposit the data and code on Zenodo.

Keywords: subtropical anticyclone, life history, wind, seabird, demographic rates

Author contribution: R.S.: conceptualization, methodology, investigation, interpretation visualization, writing—original draft; E.R.: methodology, investigation, interpretation; H.W.: data curation, interpretation; C.B.: funding acquisition, project administration, data curation, interpretation; K.D.: project administration, data curation, interpretation; C.C.U.: conceptualization, methodology, interpretation, funding acquisition; S.J.: conceptualization, methodology, interpretation, funding acquisition, project administration, data curation. All authors contributed to the writing and editing, provided final approval for publication, and accepted responsibility for the work conducted.

Abstract

Subtropical anticyclones are semi-permanent high-pressure systems located in all the major ocean basins and associated with large-scale wind and weather conditions. These systems structure the physical environments for many wildlife species, affecting ecosystem productivity, yet, their demographic impacts on wildlife species remain unexplored. Hence, it is necessary to understand whether these large-scale systems can drive critical life-history traits. Using 39 years of long-term monitoring data, we demonstrate that variability in the Indian Ocean subtropical anticyclone, the Mascarene High, affects the survival and reproduction of a marine top predator, the wandering albatross (*Diomedea exulans*). Climate analysis reveals the mechanisms behind this effect: an intensified and poleward-shifted Mascarene High enhances westerly winds, creating favorable wind conditions that increase vital rates across the entire life cycle of wandering albatrosses, including juveniles and adults, females and males. By integrating climate analyses with demographic processes, this study highlights how characteristics of subtropical anticyclones offer new insights into the influence of large-scale atmospheric features on species responses, advancing our understanding of the effects of climate variability and change on biodiversity.

Significance: *Winds influence the movement and energy use of many species. Subtropical anticyclones shape wind patterns in subtropical regions, potentially influencing wildlife population dynamics. However, we lack direct evidence linking subtropical anticyclones to the survival and reproductive rates of wildlife species. We show that an intensified and poleward-shifted Indian Ocean subtropical anticyclone enhances westerly winds, improving the survival and reproduction of wandering albatrosses, "the wind rider", breeding in the southern Indian Ocean. Our findings underscore the value of tracking subtropical anticyclone characteristics as climate indices for linking regional wind conditions to demography, providing key insights into the impacts of global change on wildlife.*

1 Introduction

Persistent large-scale rotating systems are ubiquitous features in the mid-latitude ocean and atmosphere (*1*, *2*). They are associated with lateral and vertical gradients in the physical structure of the ocean and atmosphere, influencing global climate patterns and ecosystems (*1*, *3*). In the ocean, subtropical ocean gyres are associated with variability in primary production (*3*, *4*) and can generate mesoscale eddies that impact the distribution and foraging behavior of marine top predators through the aggregation and retention of prey (*5*, *6*). Although direct effects on population dynamics have not been demonstrated, these persistent large-scale cyclonic and anticyclonic features in both the ocean and atmosphere influence winds, oceanographic conditions, and food availability, potentially impacting the survival and reproduction of wild populations.

In the atmosphere, subtropical anticyclones are semi-permanent high-pressure systems that span approximately 40% of the Earth's surface, centered around 30° latitude in both the Northern and Southern Hemispheres (*1*). They connect the mid-latitude westerly regime and tropical easterly trade winds through anticyclonic atmospheric circulation (*7*). Variability in their location and intensity drives changes in wind direction and speed. Subtropical anticyclones thus have the potential to influence demographic rates in wild species that respond to wind variability through behavior and physiology, as many species adjust their behavior to enhance foraging efficiency and conserve energy (*8*–*10*). Furthermore, winds can influence predator-prey interactions by shifting prey distribution (*11*). Subtropical anticyclones could also shape the demographic rates of wild populations through bottom-up mechanisms. Indeed, changes in wind associated with subtropical anticyclones influence the intensity of oceanic Ekman upwelling, impacting primary production and resource aggregation (*12*, *13*). Furthermore, mid-latitude weather systems in both hemispheres are closely linked to anticyclone variability through its influence on atmospheric blocking, regional winds (*14*), sea surface temperature (*15*), and precipitation (*16*), all of which impact large-scale primary production and drive bottom-up effects across trophic levels.

Subtropical anticyclones can influence a wide range of taxa. Winds on the west coast of North

America are primarily affected by the North Pacific High, and winds have been shown to impact the survival of Nearctic-neotropical migrating yellow warbler (*Setophaga petechia*) (*17*). Variability of the North Pacific High also drives biological responses in the California Current system (*18*), and winds have been linked to the distribution and abundance of blue whales (*Balaenoptera musculus*) through bottom-up effects (*19*). Furthermore, the Azores High and South Pacific High are also linked to highly productive eastern boundary upwelling systems, namely the Canary Current and Humboldt Current systems (*20*, *21*). Thus, subtropical anticyclones can affect population dynamics through a combination of winds and bottom-up mechanisms. This highlights the complex interplay between biology and physical processes, emphasizing the importance of studying the impacts of subtropical anticyclones across taxa and regions.

The subtropical anticyclones may encapsulate environmental variability in the coupled ocean-atmosphere system that is challenging to link directly to demographic patterns. This aligns with the advantage of using large-scale climate indices, which aggregate environmental conditions and have been used extensively to provide a comprehensive understanding of ecological and demographic responses to environmental variability (*22*). Unlike widely studied climate modes, such as the North Atlantic Oscillation (NAO) and El Niño–Southern Oscillation (ENSO), which have readily available predefined indices (*23*, *24*), subtropical highs lack standardized indices. Instead, climatologists often develop custom approaches to describe subtropical anticyclones based on specific research objectives (*1*, *7*). The limited investigation of subtropical anticyclones in ecology likely arises from the perceived complexity of quantifying the variability of these high-pressure systems.

Here, we use indices describing the variability in the strength and location of a subtropical anticyclone system, and test its impacts on the life-history traits of a marine top predator. We utilize a 39-year (1980-2018) capture-mark-recapture dataset of a wandering albatross (*Diomedea exulans*) population breeding in the southern Indian Ocean, a region heavily influenced by the Mascarene High (MH), the South Indian Ocean subtropical anticyclone. The wandering albatross is one of

the most wide-ranging pelagic seabirds, known for utilizing wind to undertake long-distance foraging trips (*25*), with strong winds enhancing their foraging efficiency (*26*, *27*). Previous research struggled to link demography with wind patterns, likely due to spatial-temporal mismatches, as albatrosses forage over vast distances. Employing subtropical anticyclone indices, which shape large-scale atmospheric and oceanographic conditions, may offer new insights into how highly mobile species respond to climate change. We apply Bayesian multi-event capture-mark-recapture models to quantify the effects of the MH on the entire life cycle of wandering albatrosses, including survival, breeding probability, and breeding success for juveniles and adults, as well as for females and males. Using climate anomaly composite analyses, we identify the mechanisms by which the subtropical anticyclone system shapes the life-history traits of this marine top predator. The goal of this study is to demonstrate the value of using a large-scale climate index reflecting subtropical anticyclone variability to investigate the impacts of changing climatic conditions on wild populations.

2 Results

2.1 Mascarene High affects survival and reproduction of wandering albatross

We examined how variations in the strength and spatial location of the MH impact the survival, breeding, and breeding success probabilities of wandering albatrosses breeding on Possession Island, Crozet (46°24'S 51°46'E) located in the southern Indian Ocean (Fig. 1). We found that both the strength and spatial location of the MH significantly influenced the vital rates of wandering albatrosses (Appendix Table S1 and S2 for full model results). An equatorward shift of the MH is associated with decreased vital rates, including a decrease in adult male survival probability (slope = -0.132, confidence f-value [f] = 97.0%), breeding probability for both females (-0.131, f = 98.3%) and males (-0.102, f = 98.1%), and juvenile male first-time breeding success (-0.102, f = 92.7%) (Fig. 1A). On the other hand, an intensified MH is positively correlated with adult male

survival (0.129, f=95.7%), breeding probability (0.105, f=97.5%), and juvenile female first-time breeding success (0.117, f=90.8%) (Fig. 1B). An eastward shift of the MH is positively correlated with increased juvenile male survival (0.205, f=95.7%) and first-time breeding success (0.135, f=96.6%) probabilities (Fig. 1C).

The effects of the MH on wandering albatrosses vary by sex and life stage (Fig. 1). Adult males are significantly influenced by the variability of the MH in terms of both breeding probability and survival, while it only affects the breeding probability of adult females. Furthermore, when comparing juveniles to adults, the MH impacts adult breeding probability without affecting breeding success, whereas it influences juvenile breeding success without impacting breeding probability.

2.2 Strength and location of the Mascarene High alter large-scale wind conditions

We investigated the mechanisms by which the intensity and location of the MH affect the vital rates of wandering albatrosses using composite anomaly analysis. First, we computed the long-term mean of climate variables to establish a reference condition representing the average climate experienced by the study species. Next, we identified years with the highest and lowest values of the ecological variables of interest, including survival, breeding probability, and breeding success, and plotted composite anomalies of climate variables for those years. These composites represent the anomalous climatic conditions during years with high or low vital rates, relative to the long-term mean conditions. Finally, by comparing differences in climate conditions between these composites, we gained insights into why some years result in higher vital rates, while others lead to lower vital rates.

First, we investigated the sea level pressure and wind conditions. Here we present only the anomaly composite analysis for adult male survival (Fig. 2), while all other results, which demonstrated similar and consistent patterns, are included in the Appendix (Fig. S2-6). Years with lower vital rate values were associated with low sea level pressure anomalies in both the subtropical and sub-

antarctic zones of the southern Indian Ocean (Fig. 2B). This indicates a weakened, equatorward, and westward shift of MH. The low sea level pressure anomaly resulted in a weaker meridional pressure gradient, leading to reduced westerly winds (Fig. 2B). Conversely, years with higher vital rates were associated with high sea level pressure anomalies in both the subtropical and subantarctic zones, along with low anomalies around 60-70°S. This increased the meridional pressure gradient in the subantarctic zone and enhanced westerly winds (Fig. 2C). Overall, an intensified, poleward, and eastward shift of the MH, enhancing the westerly wind belt through an increased meridional pressure gradient, is associated with higher survival, breeding, and breeding success probabilities (Fig. 2D, Appendix Fig. S2-6).

2.3 Bottom-up effects

We investigated potential bottom-up mechanisms using anomaly composite analysis for sea surface temperature (SST), wind-driven Ekman upwelling, and primary production. Higher SSTs often correlate with reduced nutrient availability (*28*), while Ekman upwelling brings nutrient-rich waters to the surface, boosting primary productivity (*29*). We found different SST anomaly patterns between adults and juvenile wandering albatrosses. In adults, years with higher male survival and breeding probability for both sexes correlated with a positive SST anomaly in the central subtropical Indian Ocean and a negative anomaly off the west coast of Australia (Fig. 3B, Appendix Fig. S2,3), coinciding with stronger winds along the eastern edge of the subtropical high (Fig. 2D). No similar pattern was detected in juveniles.

Both adult and juvenile years with higher vital rates (excluding juvenile male survival) showed a higher temperature gradient between the Agulhas Return Current and the subtropical fronts (Fig. 3A,B, Appendix Fig. S2-6). Years with higher adult male survival, female breeding probability, and juvenile male survival also showed positive upwelling anomalies in the zonal regions of 30-40°S and 50-70°S, and negative anomalies around 40-50°S (Fig. 3C, Appendix Fig. S3, 4). For both juveniles and adults, years with higher vital rates featured positive anomalies in primary

production in the region between the Agulhas Return Current and subtropical fronts (Fig. 3A,D, Appendix Fig. S2-6).

3 Discussion

Subtropical anticyclones influence large-scale wind and weather conditions, with significant implications for ecosystems. Here, we show that variability in the location and intensity of the Indian Ocean subtropical anticyclone, the Mascarene High (MH), influences vital rates across the entire life cycle of wandering albatrosses breeding on a sub-Antarctic island south of the MH. Specifically, an intensified, poleward, and eastward-shifted enhances westerly winds (Fig. 4), creating conditions favorable for dynamic soaring (*30*), and shaping demographic outcomes in juveniles and adults, with differences between sexes. These results underscore the importance of large-scale atmospheric systems in structuring marine predator populations and highlight subtropical anticyclones as potential drivers for understanding life history and population responses to climate variability.

Wandering albatrosses rely heavily on wind energy for dynamic and slope soaring (*25*). This population of wandering albatrosses forages south of the MH, within the westerlies, with females and juveniles ranging slightly farther north than males (*31*). Both an intensified and poleward-shifted MH manifest as an enhanced meridional pressure gradient, compressing and poleward displacing the westerly wind belt and enhancing overall wind conditions across the southern Indian Ocean (Fig. 4). And changes in the meridional component of the subtropical anticyclone center have been shown to be particularly affecting mid-latitude westerly winds (*13*). An eastward shift of the MH moves the high-pressure center further from Crozet, enhancing winds near the colony.

The MH variability may also influence the life-history traits through bottom-up mechanisms. A stronger and poleward-shifted MH intensifies westerly winds, which can enhance Ekman upwelling and deepen mixed layers. Furthermore, these intensified westerly winds, along with in-

creased trade winds, are likely to increase wind-stress curl across the Indian Ocean. This is associated with stronger pressure gradients between the tropics and subtropics, promoting enhanced large-scale circulation and eddy propagation. As the western boundary current of the southwest Indian Ocean, the Agulhas Current also transports nutrients from the low-latitude tropics to the nutrient-limited subtropical and subpolar gyres in subsurface "nutrient streams" (*32*). The enhanced induction of these nutrients into the mixed layer of the gyres fuels primary production in the western part of the southern Indian Ocean. Additionally, variability in the MH affects rainfall and wind patterns over southern and eastern Africa (*33*). This influences the transport of dust aerosols containing essential nutrients, deposited into nutrient-limited ocean surfaces and boosting primary production (*34*).

The reproductive responses of juveniles and adults to MH variability are different, reflecting life-history strategies. While MH variability primarily influences breeding probability in adults recovering from prior reproductive efforts, it affects breeding success in first-time breeders due to their inexperience. Previously bred adults must recover from their prior breeding attempt, which is highly reliant on environmental conditions (*35*). Thus, MH primarily affects adults by influencing breeding decisions, as experienced breeders are better equipped to handle harsh conditions during the breeding season. For first-time breeders, the initiation of their first breeding attempt relies on establishing a partnership. After fledging, they stay at sea for up to seven years before returning to their natal colony, where they begin breeding after several years of visits to bond with a partner (*36*). The onset of breeding is delayed until their body condition is optimal and a partnership is formed (*37*), and juvenile breeding probability is primarily influenced by age (*38*). Once breeding begins, the MH affects first-time breeding success due to their lack of foraging efficiency, limited physiological reserves, and unfamiliarity with their partner, all of which make them more vulnerable to environmental fluctuations and less capable of successfully raising offspring (*37*).

Adult male wandering albatrosses are more affected by variability of MH than females. While MH influences both survival and breeding probability in males, it only affects breeding probability

in females, likely reflecting sex-specific differences in the benefits of certain climate conditions. Wandering albatrosses are sexually dimorphic, with males being 20% larger in mass and having a longer wingspan than females (*39*). Their greater body mass results in higher energy expenditure during takeoff, making them more dependent on strong winds (*40*). Additionally, adult males travel further, cover broader areas, and migrate more poleward, making them more influenced by westerly winds (*26*, *39*). This higher foraging effort by males may come at a survival cost, particularly in unfavorable wind conditions, and sex-specific foraging pattern responses to wind conditions have been observed across many seabird species (*41*, *42*).

We demonstrated the importance of developing climate indices grounded in a thorough understanding of atmospheric and oceanographic dynamics, achieved by leveraging data and collaboration between ecology and climate sciences. A mechanistic understanding that goes beyond simple statistical correlations is essential for interpreting ecological responses, as many studies rely on correlations with climate variables without accounting for the underlying physical mechanisms driving these relationships. As highlighted in Mesquita *et al.* (*43*), relying on simplified proxies without comprehending the underlying physical mechanisms can obscure the complex interactions between climate variability and ecological processes.

Our subtropical anticyclone indices, which effectively capture variability in wind distribution and intensity, exemplify how a well-defined atmospheric index can reveal large-scale wind patterns and their cascading effects on ecosystems. Wind variability has recently emerged as a crucial driver of animal behavior and physiology (*10*), yet quantifying its impact on fitness and population dynamics remains challenging, likely due to mismatches in spatial-temporal scales. Demographic processes such as survival and reproduction are typically assessed annually, whereas the ecological mechanisms linking wind variability to behavior and physiology operate on much shorter timescales, from hours to days (e.g., in insect (*8*, *44*), mammal (*45*, *46*), and bird species (*47*)). Additionally, spatial scales differ markedly. Like albatrosses, many wind-affected species, such as blue whales (*19*) and common noctules (*Nyctalus noctula*) (*48*), travel thousands of kilometers an-

nually, complicating the link between local wind conditions and demographic rates. The reliance on multi-month wind averages, which correlate with large-scale annual demographic rates, may obscure underlying ecological mechanisms. Indices derived from subtropical anticyclones can help bridge this gap by capturing the dominant drivers of these relationships, filtering out noise from short-term variability, and providing a clearer understanding of how wind patterns influence population dynamics.

Moreover, the subtropical anticyclone indices link atmospheric circulation with surface wind dynamics and bottom-up processes, which are critical in many wind-driven systems. In the California Current System, influenced by the North Pacific High, blue whales track intensified wind-driven upwelling and more aggregated krill population (*19*). Incorporating North Pacific High indices may improve the predictability of blue whale presence and inform strategies to mitigate collision risks. Similarly, the Azores High influences Atlantic trade winds (*49*), which in turn regulate prey availability for Eleonora's falcons (Falco eleonorae) and affect their breeding success (*11*). Additionally, subtropical anticyclones also found to be a great predictor for the frequency of storms (*50*). Given that many pelagic seabird species respond to storms (*51*), subtropical anticyclone indices may also serve as a valuable tool for predicting storm-driven population dynamics in these species.

Each of the five subtropical anticyclone systems in the world's oceans regulates the physical environment of distinct and expansive ecosystems. Observations and climate models indicate that these systems have strengthened and shifted poleward over the 20th century, a trend projected to continue in the 21st century (*12*, *49*, *52*, *53*). Given the robustness of the signal in both past and future projections, incorporating subtropical anticyclone systems into ecological models can enhance ecological forecasts, supporting ecosystem management and conservation under climate change.

The MH indices exemplify how integrating climate variability across temporal and spatial scales can elucidate the mechanisms linking atmospheric processes to demography. By reducing noise in species' responses to environmental changes, the index enhances predictability and provides a

versatile tool for ecological research and conservation. Looking ahead, extending the application of subtropical anticyclone indices to other wind-driven systems will enable more robust projections of ecological responses under climate change, advancing both scientific understanding and conservation.

4 Materials and methods

4.1 Study system and data collection

Wandering albatrosses forage in subantarctic and subtropical waters between latitudes 30° S and 60° S while breeding (*26*), and show a wide distribution in the Southern Ocean during the non-breeding period (*54*), mainly feeding on fish and squid. Our study population of wandering albatrosses breed on Possession Island, Crozet (46°24'S 51°46'E) where a capture-mark-recapture (CMR) program has been undertaken since 1966. Fledglings and adults are banded annually using individually coded stainless-steel leg rings. Reproductive status was determined during the breeding season. Between January and February after egg laying, nests are visited three to four times to identify breeding individuals. Chicks are ringed in September and October before fledging. Breeding success is determined based on chick survival until fledging. Unmarked individuals found at the colony are also ringed each year. Sex is identified based on morphology and genetic assessment (*54*). In this study, we relied on data collected from 1980 to 2018, totaling 11584 individuals.

4.2 Mascarene High indices

The Mascarene High (MH), located in the southern Indian Ocean, is a semi-permanent subtropical anticyclone system with the potential to influence weather and climate over broader regions. Therefore, in this study, we examined how variations in MH characteristics impact the vital rates of our study species, focusing on changes in MH intensity and location (latitude and longitude). We utilized monthly reanalyzed sea level pressure data from ERA5 to calculate MH indices (*55*).

The MH area was defined as the total area within the region 30°E–120°E and 20°S–50°S above a sea level pressure of 1020.0 millibars contour (Appendix Fig. S1). The center of the MH is identified as the location with the highest sea level pressure within the MH area. The MH strength refers to the average sea level pressure value within the 1020.0 millibars contour, and the latitude and longitude of the MH center represent the spatial location of the MH (Appendix Fig. S1).

4.3 Bayesian multi-state capture-mark-recapture model (MSCMR)

We used the same Bayesian MSCMR model as in Van de Walle *et al.* (*56*) to estimate survival, breeding probability, and breeding success probability of wandering albatrosses. In a life cycle of wandering albatrosses, individuals move between a set of states over a time step of a year, conditional on transition probabilities. The wandering albatross states depend on age classes and reproductive status. All vital rates vary with age and states and we followed the definitions in Van de Walle *et al.* (*56*). More details on the Bayesian MSCMR analyses can be found in Appendix Section S1.

We then investigate the effects of the MH on vital rates. For survival probability, we used the average MH conditions from January to December. For breeding probability, we tested the effects of MH from September to December, prior to egg laying. For breeding success, we used MH conditions from January to October, covering both incubation and chick-rearing periods. We investigated the linear effect of MH indices on each demographic rate as an additive temporal covariate. All covariates were detrended and normalized prior to analysis.

4.4 Climate anomaly composite analysis

We used monthly reanalyzed sea surface temperature, sea level pressure, and surface wind data from ERA5 (*55*). Primary production, measured as the vertical integral of total carbon fixation between 0 and 100 m depth, was extracted from the Japanese 55-year Reanalysis (JRA-55) (*57*). Ekman upwelling was calculated following Kessler (*58*) using wind data. For each vital rate, low

anomaly composites were calculated by averaging conditions during the 10 years with the lowest values and subtracting the overall mean conditions for the study period. Similarly, high anomaly composites were calculated by averaging conditions during the 10 years with the highest values and subtracting the overall mean conditions. Significance was assessed using bootstrapping. Specifically, 10 years of data were randomly drawn 1,000 times, and mean conditions were subtracted to create a distribution. Statistical significance was determined based on the 90th percentile of this distribution. The significance of the difference between high and low anomaly composites was evaluated by randomly dividing the data into two groups of 10 years, subtracting each other, and repeating this process 1,000 times. The 90th percentile of the resulting distribution was used to determine significance.

5 Ethics

Licences and permissions for capture and handling of animals were granted by the Ethic Committee of Institut Polaire Francais (IPEV) and by the Préfet of Terres Australes et Antarctiques Francaises (TAAF) after advice from the Comite´ de l'Environnement Polaire (CEP).

6 Acknowledgments

This work was supported by the National Science Foundation (NSFGEO-NERC 1951500 and NSF-ORCC 2222057 to SJ, RJ, and ER), Woods Hole Oceanographic Institution under the *Joint Initiative Awards Fund from the Andrew W. Mellon Foundation* (to SJ and CCU), the *James E. and Barbara V. Moltz Fellowship for Climate-Related Research* (to CCU) and the Independent Research and Development Program (to CCU). RS thanks Joanie Van de Walle and Francesco Ventura for thoughtful discussions and comments. We acknowledge all the field workers involved in long-term demographic studies since 1960 on Possession Island for their invaluable help with data collection and Dominique Joubert for help with data management, as part of Project 109, "Seabirds and marine mammals as sentinels of global changes in the Southern Ocean: eco-evolutionary

trends and processes," funded by the French Polar Institute Paul-Émile Victor (IPEV; PI C. Barbraud). We acknowledge IPEV, Terres Australes et Antarctiques Françaises, and Zone Atelier Antarctique et Terres Australes (CNRS) for logistical and financial support. This study is part of the long-term Studies in Ecology and Evolution (SEE-Life) program of the CNRS and a contribution to Project SENSEI (Sentinels of the sea ice) funded by Fondation BNP Paribas.

References

1. M. J. Rodwell, B. J. Hoskins, *Journal of Climate* **14**, 3192–3211 (2001).
2. A. Chaigneau, A. Gizolme, C. Grados, *Progress in Oceanography* **79**, 106–119 (2008).
3. E. Di Lorenzo *et al.*, *Geophysical Research Letters* **35** (2008).
4. C. R. McClain, S. R. Signorini, J. R. Christian, *Deep Sea Research Part II: Topical Studies in Oceanography* **51**, 281–301 (2004).
5. M. C. Arostegui, P. Gaube, P. A. Woodworth-Jefcoats, D. R. Kobayashi, C. D. Braun, *Nature* **609**, 535–540 (2022).
6. I. M. Suthers *et al.*, *Limnology and Oceanography* **68**, 1019–1036 (2023).
7. T. Miyasaka, H. Nakamura, *Journal of Climate* **23**, 2115–2130 (2010).
8. G. Hennessy *et al.*, *Animal Behaviour* **161**, 23–31 (2020).
9. M. Wijers *et al.*, *Behavioral Ecology* **33**, 1180–1187 (2022).
10. L. H. Thorne, T. A. Clay, R. A. Phillips, L. G. Silvers, E. D. Wakefield, *Marine Ecology Progress Series* **723**, 73–117 (2023).
11. L. Gangoso *et al.*, *Journal of Animal Ecology* **89**, ed. by A. Fayet, 2631–2643 (2020).
12. S. J. Bograd *et al.*, *Annual Review of Marine Science* **15**, 303–328 (2023).
13. R. R. Rykaczewski *et al.*, *Geophysical Research Letters* **42**, 6424–6431 (2015).
14. M. Stowasser, Y. Wang, K. Hamilton, *Journal of Climate* **20**, 2378–2396 (2007).
15. P.-H. Chung, C.-H. Sui, T. Li, *Journal of Geophysical Research: Atmospheres* **116** (2011).
16. W. Li, L. Li, R. Fu, Y. Deng, H. Wang, *Journal of Climate* **24**, 1499–1506 (2011).

17. A. Drake, C. A. Rock, S. P. Quinlan, M. Martin, D. J. Green, *PLOS ONE* **9**, e97152 (2014).

18. I. D. Schroeder *et al.*, *Geophysical Research Letters* **40**, 541–546 (2013).

19. J. P. Ryan *et al.*, *Ecology Letters* **25**, 2435–2447 (2022).

20. E. D. Barton *et al.*, *Progress in Oceanography* **41**, 455–504 (1998).

21. R. Mogollón, P. H. R. Calil, *Global Change Biology* **24**, 3187–3198 (2018).

22. N. C. Stenseth *et al.*, *Proceedings of the Royal Society of London. Series B: Biological Sciences* **270**, 2087–2096 (2003).

23. J. W. Hurrell, Y. Kushnir, G. Ottersen, M. Visbeck, in *Geophysical Monograph Series*, ed. by J. W. Hurrell, Y. Kushnir, G. Ottersen, M. Visbeck (Washington, D. C., 2003), vol. 134, pp. 1–35.

24. M. J. McPhaden, S. E. Zebiak, M. H. Glantz, *Science* **314**, 1740–1745 (2006).

25. P. L. Richardson, *Progress in Oceanography* **88**, 46–58 (2011).

26. H. Weimerskirch, M. Louzao, S. d. Grissac, K. Delord, *Science* **335**, 211–214 (2012).

27. T. Cornioley, L. Börger, A. Ozgul, H. Weimerskirch, *Journal of Animal Ecology* **85**, 1318–1327 (2016).

28. M. J. Behrenfeld *et al.*, *Nature* **444**, 752–755 (2006).

29. C. F. P, *Upwelling in the Ocean : Modern Processes and Ancient Records* (1995).

30. P. L. Richardson, E. D. Wakefield, R. A. Phillips, *Movement Ecology* **6**, 3 (2018).

31. H. Weimerskirch *et al.*, *Journal of Experimental Marine Biology and Ecology* **450**, 68–78 (2014).

32. J. L. Pelegrí, G. T. Csanady, *Journal of Geophysical Research: Oceans* **96**, 2577–2583 (1991).

33. D. Manatsa, Y. Morioka, S. K. Behera, C. H. Matarira, T. Yamagata, *Climate Dynamics* **42**, 1259–1274 (2014).

34. J. A. Gittings *et al.*, *PNAS Nexus* **3**, pgae386 (2024).

35. H. Weimerskirch, *J Anim Ecol* **87**, 945–955 (2018).

36. H. Weimerskirch, Y. Cherel, F. Cuenot-Chaillet, V. Ridoux, *Ecology* **78**, 2051–2063 (1997).

37. H. Weimerskirch, *Oikos* **64**, 464–473 (1992).

38. R. Fay, C. Barbraud, K. Delord, H. Weimerskirch, *Ecology* **97**, 1842–1851 (2016).

39. S. A. Shaffer, H. Weimerskirch, D. P. Costa, *Functional Ecology* **15**, 203–210 (2001).

40. T. A. Clay *et al.*, *Journal of Animal Ecology* **89**, 1811–1823 (2020).

41. S. Lewis, R. A. Phillips, S. J. Burthe, S. Wanless, F. Daunt, *Journal of Animal Ecology* **84**, 1490–1496 (2015).

42. E. D. Wakefield *et al.*, *Ecological Monographs* **79**, 663–679 (2009).

43. M. d. S. Mesquita *et al.*, *Frontiers in Ecology and Evolution* **3** (2015).

44. A. M. Alma, A. G. Farji-Brener, L. Elizalde, *The American Naturalist* **190**, 410–419 (2017).

45. R. R. Togunov, A. E. Derocher, N. J. Lunn, *Scientific Reports* **7**, 46332 (2017).

46. S. Renda, S. Périquet, A. le Roux, *Mammal Research* **68**, 215–221 (2023).

47. C. Saraux, A. Chiaradia, M. Salton, P. Dann, V. A. Viblanc, *Ecological Monographs* **86**, 61–77 (2016).

48. E. Hurme, I. Lenzi, M. Wikelski, T. A. Wild, D. K. N. Dechmann, *Science* **387**, 97–102 (2025).

49. N. Cresswell-Clay *et al.*, *Nature Geoscience* **15**, 548–553 (2022).

50. B. Wang, B. Xiang, J.-Y. Lee, *Proceedings of the National Academy of Sciences* **110**, 2718–2722 (2013).

51. H. Weimerskirch, A. Prudor, *Scientific Reports* **9**, 5400 (2019).

52. W. Li *et al.*, *Geophysical Research Letters* **40**, 5959–5964 (2013).

53. B. C. Backeberg, P. Penven, M. Rouault, *Nature Climate Change* **2**, 608–612 (2012).

54. H. Weimerskirch, J. Lallemand, J. Martin, *Journal of Animal Ecology* **74**, 285–291 (2005).

55. H. Hersbach *et al.*, *Quarterly Journal of the Royal Meteorological Society* **146**, 1999–2049 (2020).

56. J. Van de Walle *et al.*, *Journal of Animal Ecology* **93**, 676–690 (2024).

57. S. Kobayashi *et al.*, *Journal of the Meteorological Society of Japan. Ser. II* **93**, 5–48 (2015).

58. W. S. Kessler, *Journal of Physical Oceanography* **32**, 2457–2471 (2002).

7 Figures

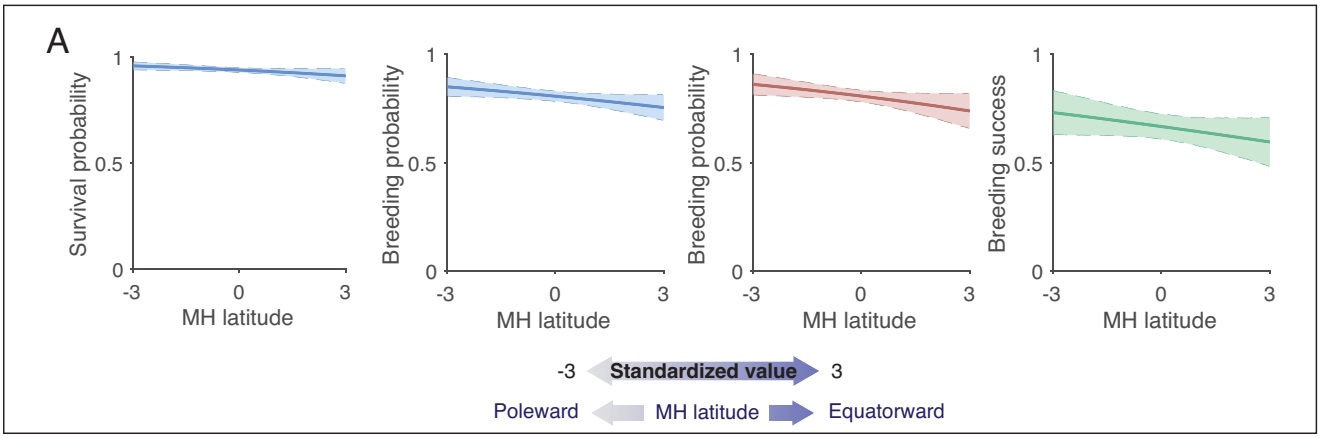
A
Survival probability
Breeding probability
Breeding probability
Breeding success
MH latitude
-3
Standardized value
3
Poleward
MH latitude
Equatorward

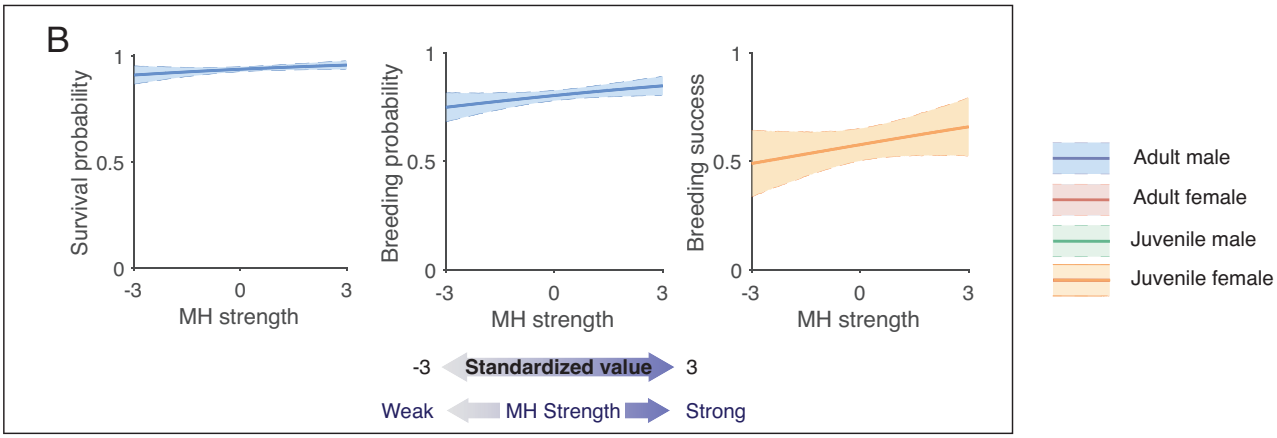
B
Survival probability
Breeding probability
Breeding success
MH strength
-3
Standardized value
3
Weak
MH Strength
Strong
Adult male
Adult female
Juvenile male
Juvenile female

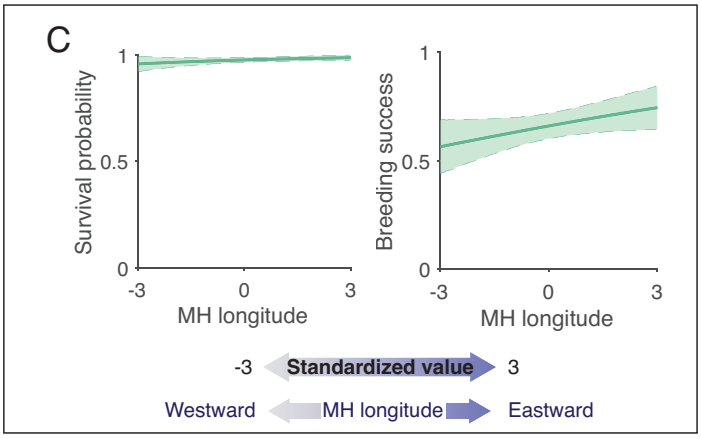
C
Survival probability
Breeding success
MH longitude
-3
Standardized value
3
Westward
MH longitude
Eastward

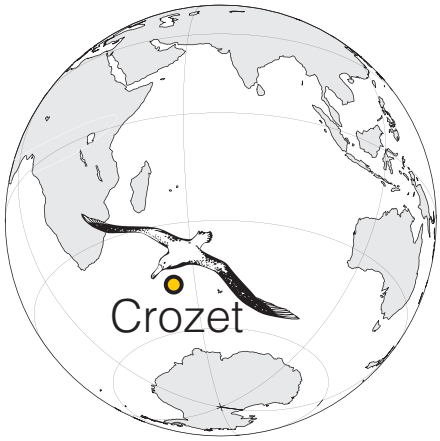
Crozet

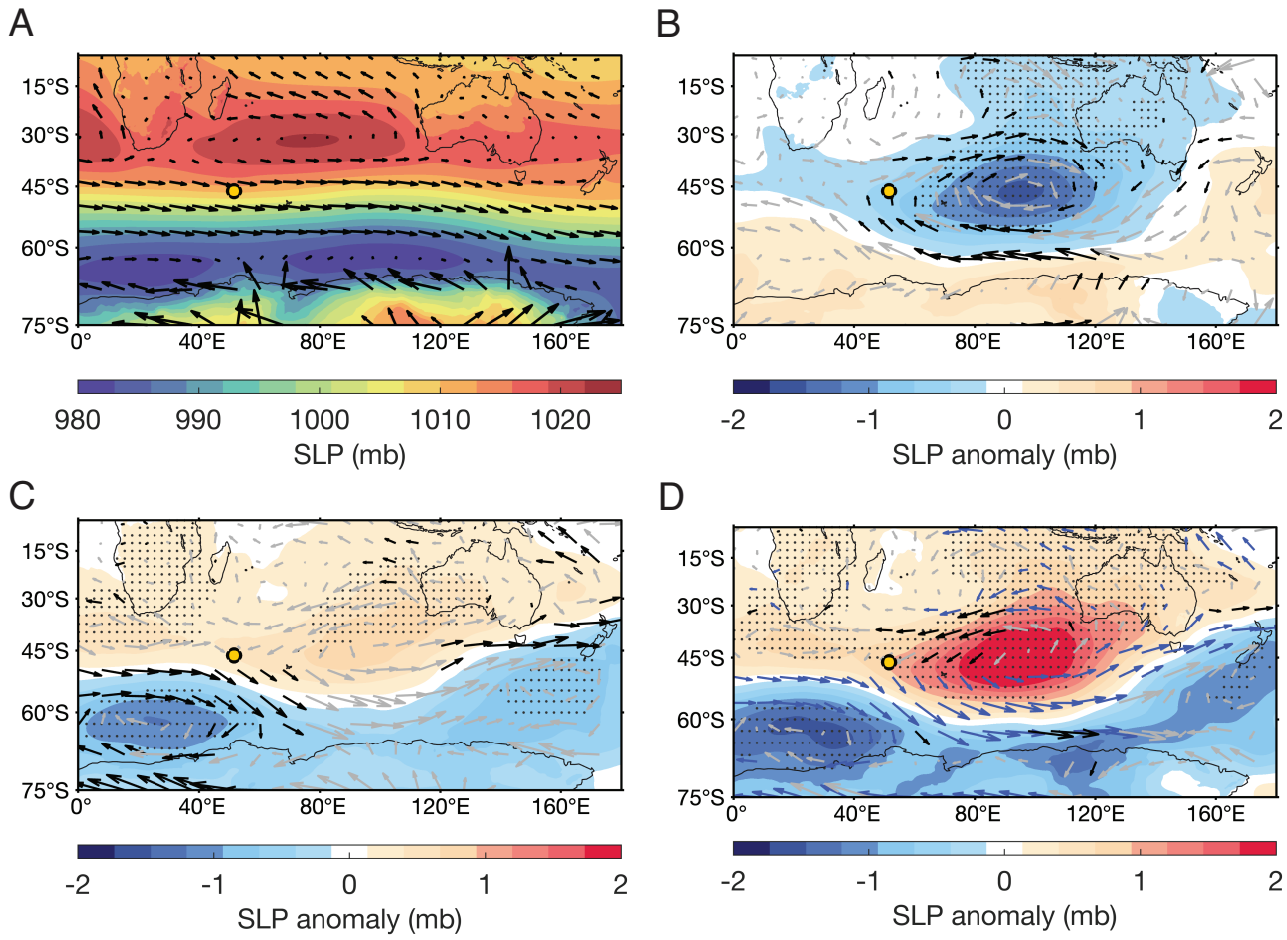
A
B
C
D
15°S
30°S
45°S
60°S
75°S
0°
40°E
80°E
120°E
160°E
980
990
1000
1010
1020
SLP (mb)
-2
-1
0
1
2
SLP anomaly (mb)

Figure 2

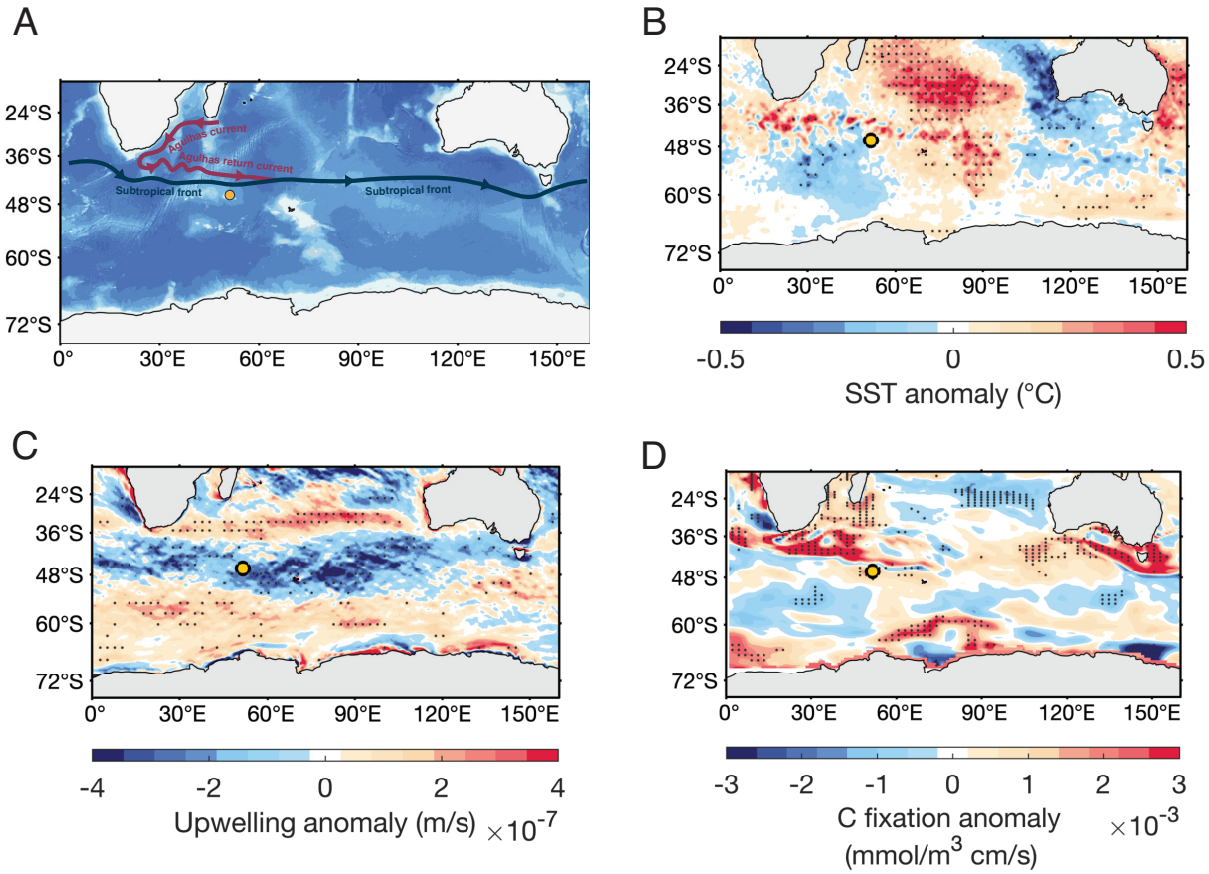
A
24°S
36°S
48°S
60°S
72°S
0°
30°E
60°E
90°E
120°E
150°E
Agulhas current
Agulhas return current
Subtropical front
Subtropical front
B
-0.5
0
0.5
SST anomaly (°C)
C
-4
-2
0
2
4
Upwelling anomaly (m/s) ×10^-7
D
-3
-2
-1
0
1
2
3
C fixation anomaly (mmol/m^3 cm/s) ×10^-3

Figure 3

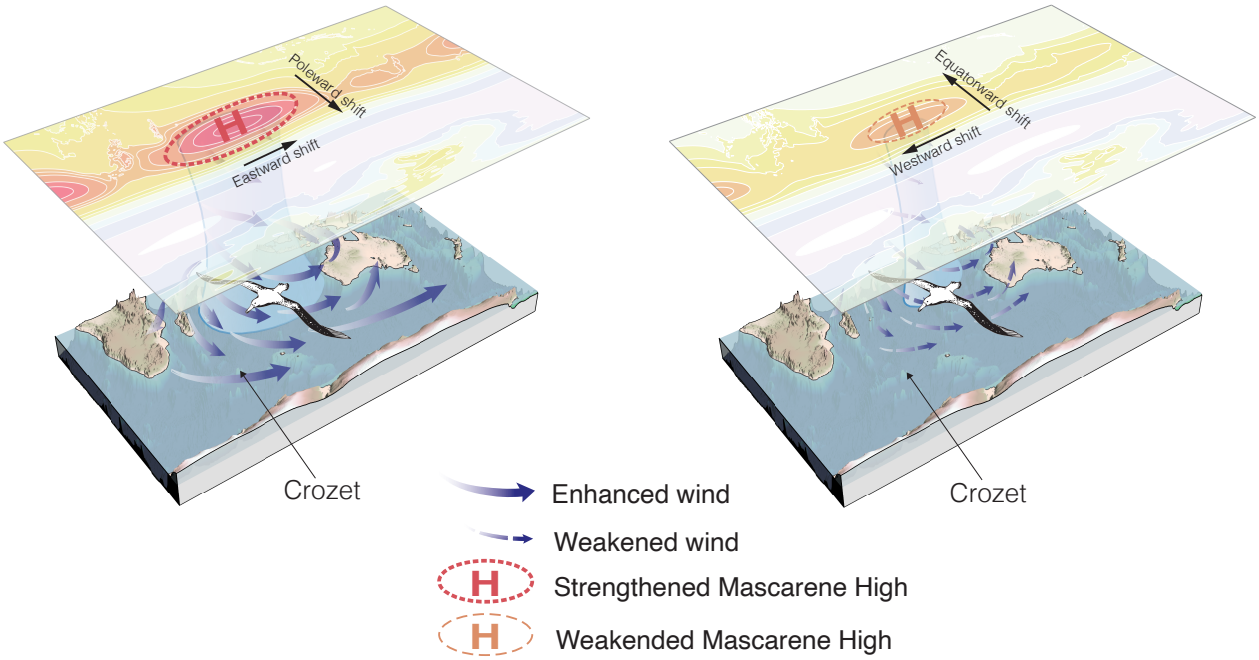

Figure 4

8 Figure legends

Figure 1. Effects of variability in Mascarene High (MH) intensity and spatial location on the life-history traits (±95%) of wandering albatrosses breeding on Crozet Island. (A) Effects of MH latitude on vital rates; (B) Effects of MH strength on vital rates; (C) Effects of MH longitude on vital rates. Note that the breeding success probability for juveniles refers to breeding success of their first breeding attempt in life. All covariates have been standardized. An increase in MH latitude indicates an equatorward shift of the center, while increased MH strength signifies an intensified MH, and increased MH longitude indicates an eastward shift of the MH center.

Figure 2. Composite anomaly analysis of sea level pressure (SLP) and wind conditions affecting the survival probability of male wandering albatrosses. (A) Long-term mean (1980-2018) of SLP and wind conditions. (B,C) Composite anomalies of SLP and winds during years with high

male survival probability (B) and years with low male survival probability (C). Black wind vectors indicate significant wind anomaly, while light gray wind vectors indicate insignificant wind anomaly. Light dotted stippling indicates significant anomaly in SLP. (D) Differences in SLP and wind conditions during composites of high and low male survival years. Black wind vectors indicate significant wind differences associated with reduced wind speed, blue wind vectors indicate significant differences with increased wind speed, and light gray wind vectors indicate insignificant differences. Light dotted stippling denotes significant differences in SLP.

Figure 3. Anomaly composite analysis of potential bottom-up mechanisms influencing male wandering albatross survival probability. (A) shows the location of key oceanographic features, such as the Agulhas Return Current and Subtropical Front. (B), (C), and (D) show differences in sea surface temperature (SST), Ekman upwelling, and primary productivity, respectively, between years of high and low male survival. Primary productivity was measured as the vertical integral of total carbon fixation between 0 and 100 m below the surface. Light dotted stippling indicates significant differences between years of higher and lower male survival probability.

Figure 4. Schematic illustrating how changes in the intensity and position of the Mascarene High affect wind conditions for wandering albatrosses breeding on Crozet. A stronger, poleward-shifted Mascarene High enhances westerly winds, creating favorable conditions that improve albatross survival and reproduction.